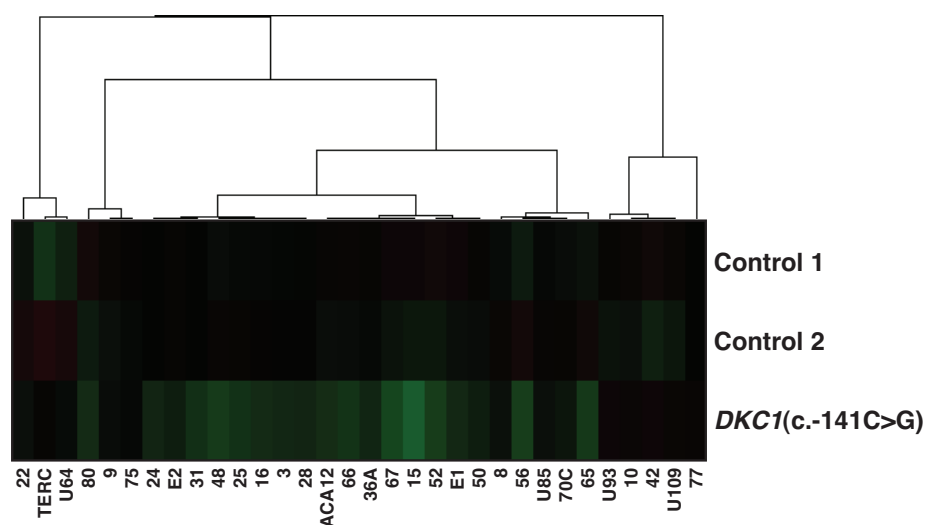


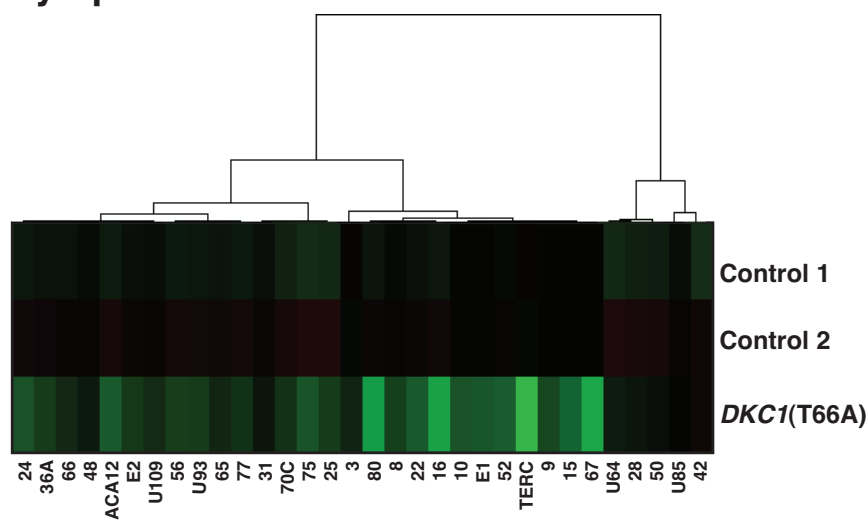
A

CD34+ cells



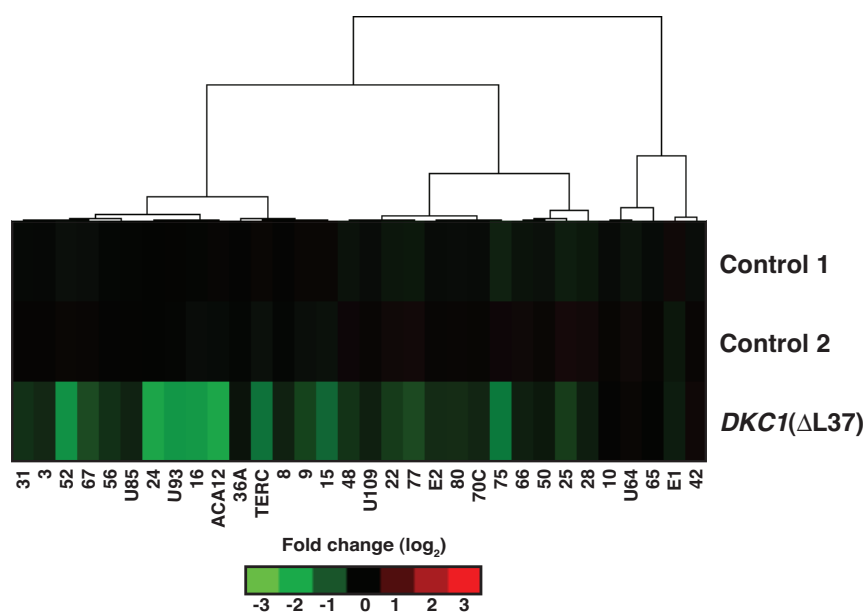
B

Lymphoblasts

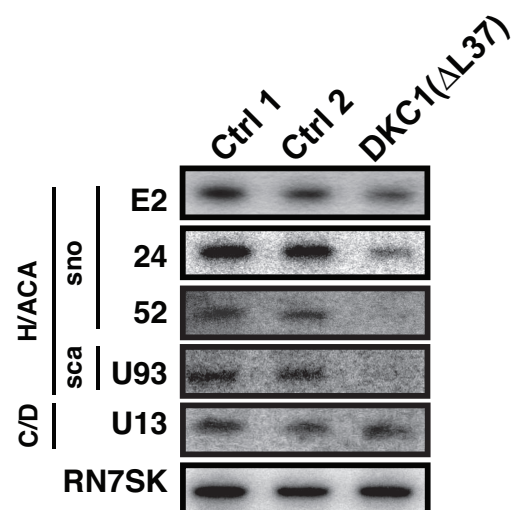


C

Fibroblasts



D



Northern blot quantification

H/ACA snoRNA to RN7SK relative to controls

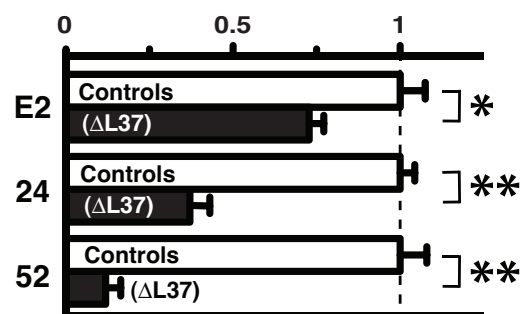
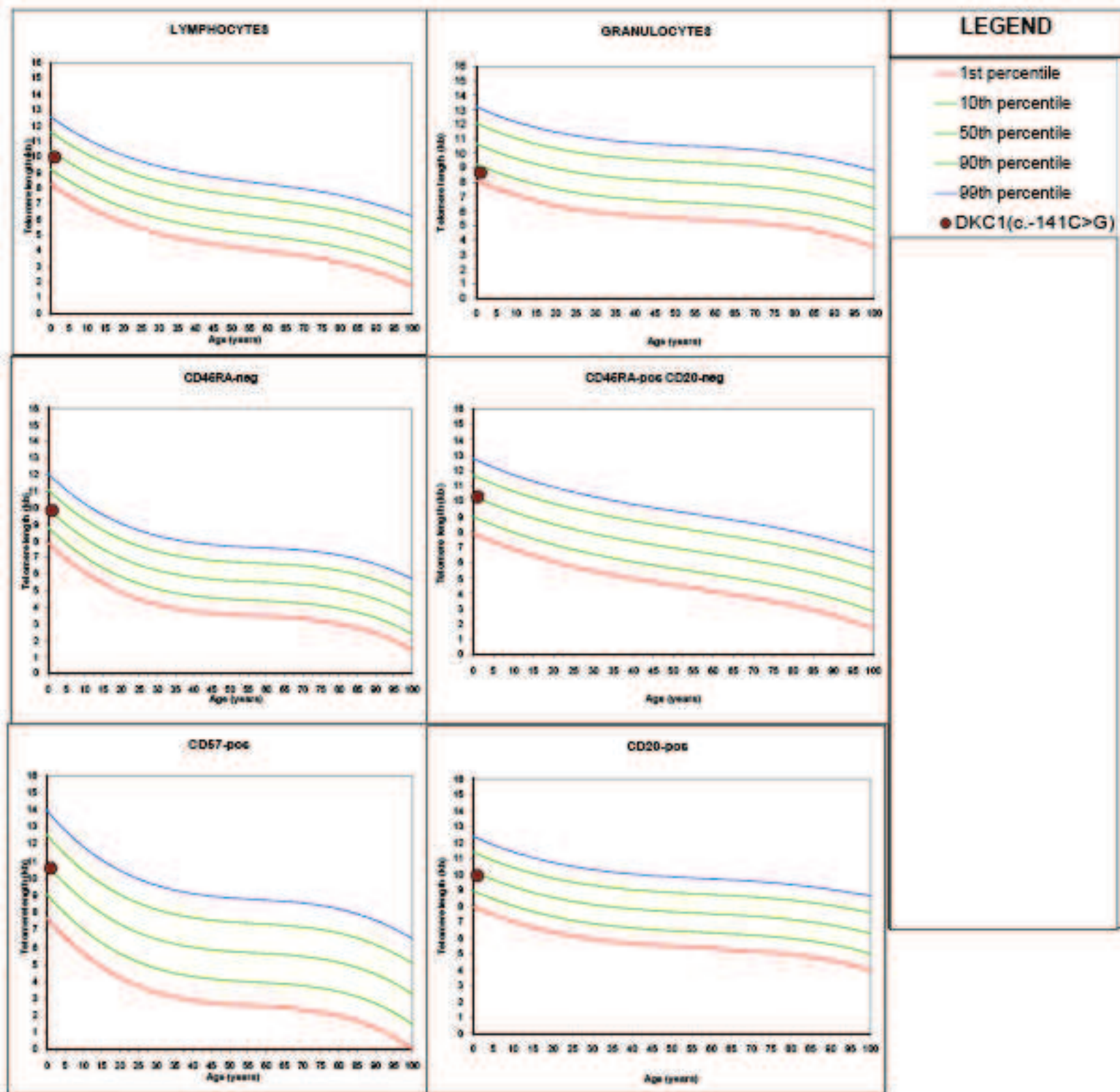


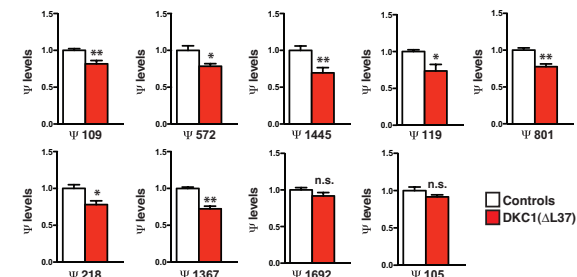
Figure S2



A

Ψ site on 18S rRNA	Corresponding guide H/ACA snoRNAs
Ψ105	snoRNA36A, snoRNA36B, snoRNA50, snoRNA76
Ψ109	snoRNA42, snoRNA80, snoRNA80B
Ψ119	snoRNA66
Ψ218	snoRNA31
Ψ572	snoRNA42, snoRNA80, snoRNA80B
Ψ801	snoRNA25
Ψ1367	snoRNA15
Ψ1445	snoRNA67
Ψ1692	snoRNA70B, snoRNA70C, snoRNA70D, snoRNA70E, snoRNA70F, snoRNA70G

B



C

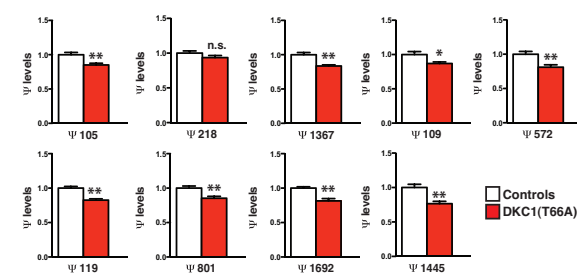
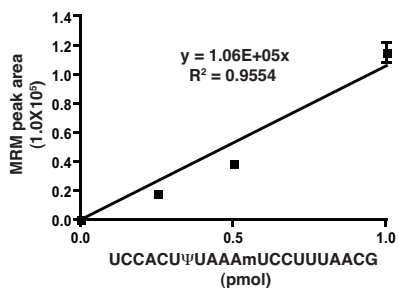
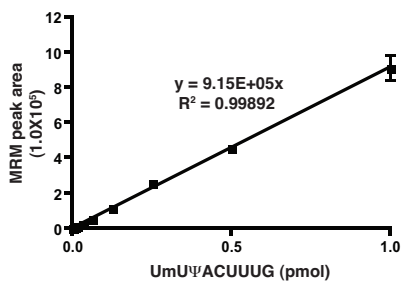
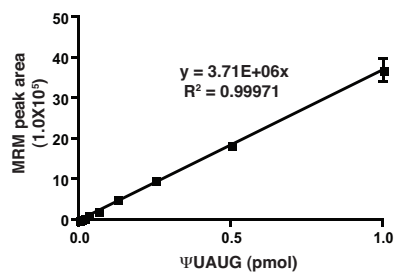
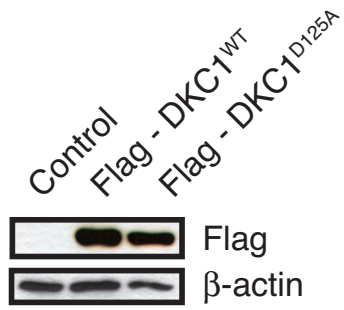


Figure S3

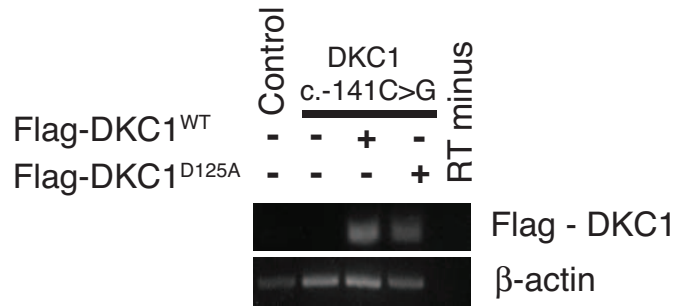
D



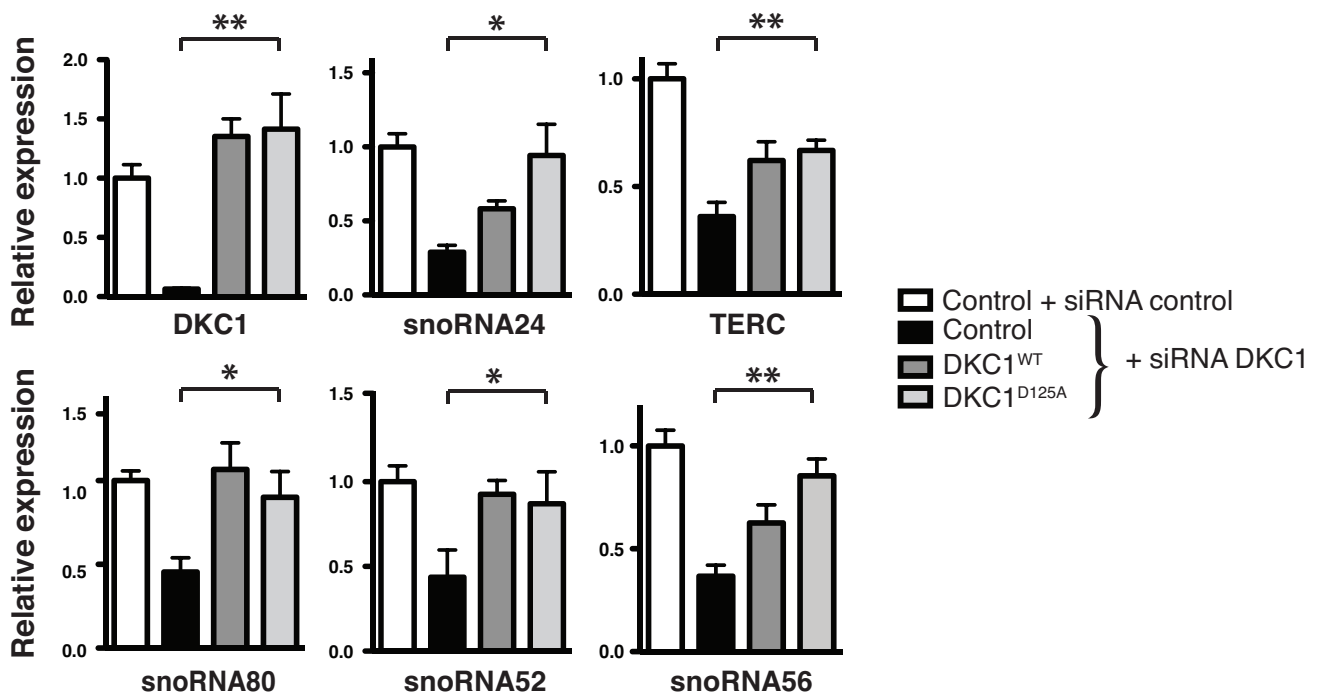
A



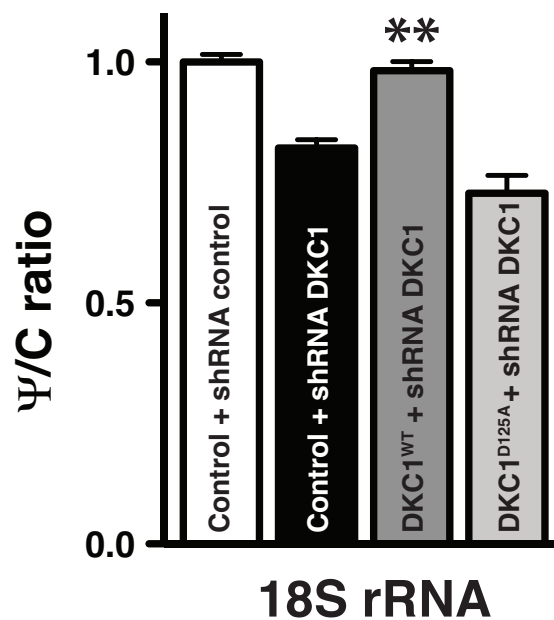
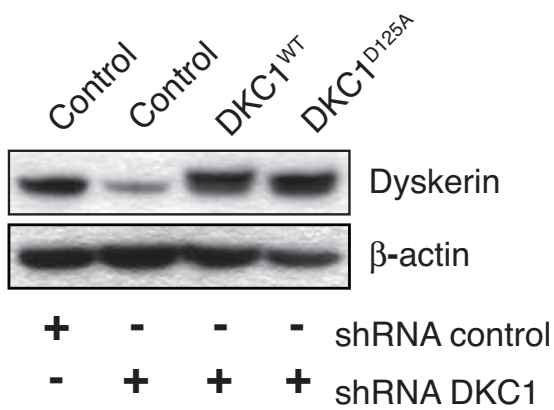
B



C



D



Supplemental Information

Extended Experimental Procedures

NCI participant lymphocytes

The patients with T70I, K314R, A353V, and K390Q mutations in *DKC1* are participants in the Institutional Review Boards (IRBs)-approved longitudinal cohort study at the National Cancer Institute (NCI) entitled “Etiologic Investigation of Cancer Susceptibility in Inherited Bone Marrow Failure Syndromes” (www.marrowsfailure.cancer.gov, NCI 02-C-0052, ClinicalTrials.gov Identifier: NCT00027274 (Alter et al., 2010)). Patients and their family members completed detailed questionnaires and underwent thorough clinical evaluations. Mutation testing of *DKC1* was done in a CLIA-certified laboratory. Patient-derived lymphocytes were immortalized with EBV using standard methods and maintained in 20% RPMI as described (Bellodi et al., 2010a).

Commercially available healthy controls and X-DC cells

Controls (GM04390 and GM00730) and *DKC1*(Δ L37) (GM01774) fibroblasts (Passage 7-10) were obtained from Coriell Cell Repositories (Coriell Institution for Medical Research, Camden, NJ) and maintained in MEM as described (Bellodi et al., 2010a). Controls (GM11626, GM07544, GM03299, GM22674, GM22647, GM08814 and GM03329) and *DKC1*(T66A) (GM03195) lymphocytes were obtained from Coriell Cell Repositories and maintained in 20% RPMI as described (Bellodi et al., 2010a).

Primary bone marrow progenitor cells

Informed consent was obtained from the *DKC1*(c.-141 C>G) patient in accordance with a human subjects study protocol approved by the IRBs of the Seattle Children’s Hospital and Fred Hutchinson Cancer Research Center. Anonymous healthy control bone marrow cells were obtained from discarded bone marrow harvest screens as approved by the Fred Hutchinson Cancer Research Center IRB.

Plasmids

A plasmid encoding *DKC1*^{WT} has previously been described (Bellodi et al., 2010b). The *DKC1*^{D125A} mutant was generated using a site-directed mutagenesis kit (Stratagene) according to manufacturer's instructions.

Western blot, northern blot, and qPCR analysis

Western blot was performed using standard protocols and the following primary antibodies: dyskerin (1:1000; Santa Cruz), FLAG (1:1000; Sigma), and β -actin (1:15,000; Sigma). Northern blot analysis was performed on total RNA (2 μ g), isolated using Trizol reagent (Invitrogen), using ³²P end labeled oligonucleotides (Table S3) and quantification was performed using ImageQuant 5.2 software (Molecular Dynamics). For real-time qPCR analysis, total RNA was isolated using Trizol Reagent and treated with Turbo DNA-free kit (Ambion). 1-2 μ g of RNA was reverse transcribed using SuperScript II Reverse Transcriptase Kit (Invitrogen) and analysis was performed using iQ Sybr Green mix (Biorad). The expression of H/ACA small RNAs was measured by real-time qPCR, relative to two type-matched control cells for each mutation, and normalized to

the abundance of RN7SK small ncRNA from at least three independent experiments. Primer sequences are listed in Table S3. Selected H/ACA snoRNAs guide Ψ modifications within functionally important regions of both the small and large ribosomal subunits such as the peptidyl transferase center (PTC), the decoding center (DC), as well as ribosome expansion segments.

HPLC and Mass Spectrometry quantification of human rRNA pseudouridylation

Global analysis of rRNA pseudouridine levels was performed by HPLC analysis on a C₁₈ 250x4.6 mm (particle size 5 μ m) Reverse phase HPLC column (Agilent) as previously described (Jack et al., 2011). For quantifications of site-specific Ψ modifications all LC/MS/MS analyses were performed using an in-house packed capillary column (320 μ m ID x 150 mm length, packed with Jupiter 4 μ m Phenomenex Proteo 90 A material). The solvents used were as described with minor modifications (Apffel et al., 1997). A stock solvent solution was made consisting of 460 ml of HPLC grade water (Fisher Scientific), 42 ml of 1,1,1,3,3,3-hexafluoro-2-propanol (Fluka) and 1.2 ml of Triethylamine (Pierce). Solvent A was prepared by diluting the stock 1:1 V:V with HPLC grade water. Solvent B was prepared by diluting the stock 1:1 V:V with HPLC grade methanol (Fisher). The HPLC system consisted of an Eldex Micropro LC and a Dionex LC-Packings FAMOS auto sampler. The flow rate was 5 to 7 μ l/min on a 45 mins linear gradient from 0-70 % B. All samples and standards were dissolved in Solvent A prior to injection. Selected Ψ sites on human 18S rRNA (Figure S3A) were determined by LC/MS/MS following RNase T1 (Roche) digestion using 10U/ μ g of gel purified 18S rRNA (0.2-1.0 μ g) in 10 mM Tris-HCl, 1 mM EDTA, pH 7.4 on a Thermo LTQ Orbitrap Velos mass spectrometer using 90 mins gradients and operated in negative ion detection mode. The IS voltage was set at 4.0 to 5.0 kV, with source temperature at 225°C and a sheath gas flow of 10. The instrument was run in a data dependent mode, using a survey scan from 400-1600, resolution 30,000, and with a 2E6 AGC setting for full scan with one microscan of 250 millisecond (ms). After every survey scan, the top three most intense ions were selected for HCD fragmentation with 2E5 AGC setting, and 3 x 200 ms microscans. The HCD mass range was set at 100-2000. Ions selected for HCD were added to an exclusion list for the next 60 secs. The data files were processed using Xcalibur software suite (Thermo Scientific). Extracted ion profiles for previously characterized Ψ ions at 165.0302 (when the Ψ is at the 5' end of an oligo) and 207.0400 (when elsewhere in the oligo) (Pomerantz and McCloskey, 2005) were created for all data files and were used to locate and map distinct Ψ -containing oligonucleotides from purified human 18S rRNA. The HCD spectrum was manually interpreted with the aid of Ariadne (Nakayama et al., 2009) and the Mongo Oligo Mass Calculator program (<http://medlib.med.utah.edu/masspec/mongo.htm>). The identifications of Ψ -containing oligonucleotides were facilitated by the accurate masses (+/- 5 ppm) obtained from the Velos instrument in both full scan and HCD scan mode. In total nine oligonucleotides containing one unique Ψ residue from human 18S rRNA were selected and the sequence of the oligonucleotides with the position of the pseudouridine highlighted in bold were the following: Ψ UAUG (Ψ 109), CCC **Ψ** UUG (Ψ 1692), UUmCC **Ψ** UUmG (Ψ 119), CA **Ψ** UUAUCAG (Ψ 218), UmU **Ψ** ACUUG (Ψ 801), **Ψ** UAAUCCG (Ψ 1367), CUCAmUUA **Ψ** AA **Ψ** CAG (Ψ 105), CCCCCAACUUmCU **Ψ** AGmAG (Ψ 1445), UCCACU **Ψ** UAAAmUCCUUUAACG (Ψ 572). Upon identification of specific Ψ sites,

relative quantitation was obtained by MRM using an ABSciex QTRAP 4000 mass spectrometer and using the same HPLC conditions described above. The appropriate parent mass determined by the Velos HCD experiments was selected for MRM analysis. The QTRAP was operated in negative ion mode, using the Turbo IonSpray source with a spray voltage of -4.5 kV, ion source gas one value of 15 and a source temperature of 50°C. The instrument was operated in LOW/LOW resolution setting for these analyses. The dwell time for each transition was set to 50 ms and the collision energy was set at 65V. The Analyst 1.5 software was used to determine the peak area for each transition. To ascertain that the MRM response of the Ψ -containing oligonucleotides was linear over the range of areas detected in patient samples, a standard curve of areas against amount injected was generated for three synthetic Ψ -containing oligonucleotides (Figure S3D). The 996 (2+ ion) to 362 transition (362 is the y1 ion for this oligo) of a non- Ψ containing oligonucleotide (AmAmCCUG) was selected as a normalization control in the analysis. The transitions used for MRM experiments and retention times for each oligonucleotide are shown in Table S4. Using this method, for a given oligonucleotide, only the presence of a Ψ ion can be determined and not the amount of the corresponding oligonucleotide devoid of Ψ . Therefore, Ψ quantification measurements are relative and not absolute. Using the experimental conditions described above, we were unable to quantify single Ψ residues present on oligonucleotides that coeluted under our HPLC conditions or on oligonucleotides containing more than one Ψ residue. However, resolution of additional Ψ sites on 18S rRNA may be achieved by employing RNA nucleases other than RNAase T1 (such as RNase A and/or U2) and/or by altering the HPLC conditions.

Methylcellulose colony forming assays

CD34+ hematopoietic progenitors were purified from total bone marrow mononuclear (BMCs) cells aspirates using CD34+ microbeads (Miltenyi Biotech) according to the manufacturer instructions. After purification, flow cytometry confirmed that the isolated cells were greater than 85% CD34+. Cells were cultured in StemSpan SFEM serum-free media (StemCell Technologies) supplemented with 100ng/ml of the following cytokines; stem cell factor (SCF), Flt3 ligand, thrombopoietin (TPO), and interleukin-6 (IL-6) and incubate overnight at 37°C. Healthy control and X-DC patient purified CD34+ cells were transfected with control, DKC1^{WT} or DKC1^{D125} expression vectors using the human CD34+ Amaxa nucleofection kit (Amaxa Biosystems). Transfected CD34+ progenitor cells were cultured as described above and plated in methylcellulose medium (Methocult H4434, StemCell Technologies) supplemented with SCF, GM-CSF, interleukin-3 (IL-3) and erythropoietin (EPO) after 12 hours. Cells were seeded at 500 cells/dish in duplicate and maintained at 37°C. Colonies containing more than 20 cells were scored using an inverted light microscope (Leica) after 10 days. All cytokines were purchased from Peprotech.

Telomere length measurements

Telomere length was measured by multicolor flow FISH (Repeat Diagnostics) as described (Alter et al., 2007; Baerlocher et al., 2006).

Supplementary Figure Legends

Figure S1. H/ACA small RNAs expression levels in controls and X-DC patient cells.

(A) Heatmap diagram showing hierarchical clustering of the mean relative expression of H/ACA small RNAs in two independent primary control and *DKCI*(c.-141C>G) CD34+ cells. (B) Heatmap diagram showing hierarchical clustering of the mean relative expression of H/ACA small RNAs in two independent controls and *DKCI*(T66A) lymphoblasts. (C) Heatmap diagram showing hierarchical clustering of the mean relative expression of H/ACA small RNAs in two independent controls and *DKCI*(Δ L37) primary fibroblasts. The expression of H/ACA small RNAs was measured by real-time qPCR from three independent experiments (Table S1-S2). Each row represents a control or X-DC patient-derived cells. Columns show individual H/ACA small RNA expression levels. The color bar indicates the color-coding of small RNA expression from +3 to -3 in \log_2 space. Statistical information is included in Table S2. (D) Northern blot analysis of the indicated small RNAs in fibroblasts from two healthy control (Ctrl1 and Ctrl 2) and *DKCI*(Δ L37) patients, with RN7SK small ncRNA used as a loading control (top). The graph shows the ratio of H/ACA snoRNA E2, snoRNA 24, and snoRNA 52 expression normalized to the levels of RN7SK in two controls and *DKCI*(Δ L37) fibroblasts from three independent experiments (bottom). Statistical analysis was performed using the unpaired Student's *t*-test, * P <0.05 and ** P <0.01.

Figure S2. Telomere length measurements in *DKCI*(c.-141C>G) patient hematopoietic cells. Telomere length was measured by multicolor flow FISH (Repeat Diagnostics) in the indicated leukocyte subsets from the *DKCI*(c.-141C>G) patient. The vertical axis represents telomere length in kilobytes. Lines indicated the first, tenth, 50th, 90th, and 99th percentiles for telomere lengths of normal control subjects. The red circle represents the *DKCI*(c.-141C>G) patient.

Figure S3. Site-specific Ψ quantifications on 18S rRNA. (A) The position of specific Ψ sites on 18S rRNA that were resolved and quantified by mass spectrometry as well as the corresponding guide H/ACA snoRNAs annotated to modify at these sites are shown. H/ACA snoRNAs analyzed in our study are highlighted in bold (see Figure 1C). (B) Site-specific quantification of Ψ levels in two controls and in *DKCI*(Δ L37) fibroblasts. Individual graphs show the mean pseudouridylation levels \pm SEM relative to two controls from three independent experiments. Statistical analysis was performed using the unpaired Student's *t*-test, * P <0.05 and ** P <0.01. (C) Site-specific Ψ quantifications in 18S rRNA from controls and *DKCI*(T66A) lymphoblasts. Individual graphs show the mean pseudouridylation levels \pm SEM relative to two controls from three independent experiments. Statistical analysis was performed using the unpaired Student's *t*-test, * P <0.05 and ** P <0.01. (D) Calibration curves were generated by LC/MS/MS analysis of synthetic Ψ -containing oligonucleotide corresponding to sequences of human 18S rRNA. For each oligonucleotide the position of the Ψ residue is indicated: Ψ UAUG (Ψ 109), UmU Ψ ACUUUG (Ψ 801), and UCCACU Ψ UAAAmUCCUUUAACG (Ψ 572). Graphs show MRM transition peak areas corresponding to concentrations ranging from 7.8 fmol to 1.0 pmol of Ψ -containing oligonucleotides. Each data point is the average \pm SEM of triplicate measurements. Data was fit to a linear regression function, where *y* represents

slope and R^2 is the correlation coefficient. All Ψ -containing oligonucleotides yielded linear calibration curves with high precision.

Figure S4. Expression and characterization of wild type and catalytically inactive dyskerin alleles. (A) 293T cells were transduced with control expression vectors or expression vectors encoding FLAG-tagged wild type (WT) dyskerin or the catalytic mutant (D125A) dyskerin. Representative western blot illustrating the levels of DKC1^{WT} and DKC1^{D125A} protein levels. β -actin was used as a loading control. (B) Semi-quantitative RT-PCR demonstrating the presence of FLAG-DKC1^{WT} and FLAG-DKC1^{D125A} mRNA levels in control and *DKC1*(c.-141C>G) CD34+ cells upon transfection with empty vector or plasmids encoding FLAG-DKC1^{WT} and FLAG-DKC1^{D125A}. β -actin mRNA expression levels were used as internal control. (C) Expression levels of DKC1 and different classes of H/ACA small RNAs was measured by real-time qPCR in HeLa cells expressing empty vector (control), DKC1^{WT} or DKC1^{D125A} following transfection with scramble or DKC1-targeting siRNA oligonucleotides as indicated (top) and previously described (Jack et al., 2011). Graphs show mean fold expression \pm SEM relative to control and normalized to the abundance of RN7SK small non-coding RNA from two independent experiments. Statistical analysis was performed using the unpaired Student's *t*-test, * P <0.05 and ** P <0.01. (D) Western blot analysis of dyskerin and β -actin (right) and HPLC quantification of 18S rRNA Ψ levels (left) in HEK293T cells stably expressing short hairpin RNA (shRNA) targeting the 3' UTR of DKC1 or a control sequence, in the absence or presence of DKC1^{WT} or DKC1^{D125A}. The graph shows mean Ψ to cytosine (Ψ /C) ratio \pm SEM relative to controls in two experiments. Statistical analysis was performed using the unpaired Student's *t*-test, ** P <0.01.